IJST, Transactions of Mechanical Engineering, Vol. 38, No. M2, pp 321-335
Printed in The Islamic Republic of Iran, 2014

EFFECT OF PHASE LAGS ON THERMOELASTIC FUNCTIONALLY GRADED MICROBEAMS SUBJECTED TO RAMP-TYPE HEATING*

A. E. ABOUELREGAL[1] AND A. M. ZENKOUR[2,3**]

[1]Dept. of Mathematics, Faculty of Science, Mansoura University, Mansoura 35516, Egypt
[2]Dept. of Mathematics, Faculty of Science, King Abdulaziz University, P.O. Box 80203, Jeddah 21589, Saudi Arabia
[3]Department of Mathematics, Faculty of Science, Kafrelsheikh University, Kafr El-Sheikh 33516, Egypt
Email: zenkour@gmail.com

Abstract– This article deals with the study of generalized solution for the vibration of functionally graded (FG) microbeam in the context of the dual phase lag model. Numerical results are presented for the FG beam subjected to a ramp-type heating and has exponentially varying material properties through the thickness. The effect of the ramping time parameter is studied on the lateral vibration, temperature, displacement, stress, the moment and the strain energy of the FG microbeam. The influence of the thickness of the beam is also analyzed. A comparison of the results for different theories is presented. The results obtained theoretically have been computed numerically and are presented graphically. Some particular cases are also discussed in the context of the problem.

Keywords– Thermoelasticity, dual phase lags, functionally graded, microbeam, ramp type heating

1. INTRODUCTION

Thermal stresses arise in many areas and have been subjects of interest. They are frequently important factors in determining material life. In coupled thermoelasticity (CTE) theory, if an elastic continuum is subjected to a mechanical or thermal disturbance, the effect of the disturbance will be felt instantaneously in both fields as governing equations are coupled. Physically, this means that a portion of the disturbance has an infinite velocity of propagation. Such behavior is physically inadmissible. Biot [1] developed the coupled theory of thermoelasticity to deal with a defect of the uncoupled theory that mechanical causes have no effect on the temperature. However, this theory shares a defect of the uncoupled theory in that it predicts infinite speeds of propagation for heat waves. This implies that the thermal wave propagates with an infinite speed, which is physically unrealistic. Lord and Shulman (LS) [2] proposed a model with one relaxation time. They aim to attempt eliminating the paradox of infinite velocity of thermoelastic disturbances inherent in the classical CTE. After a few years, Green and Lindsay (GL) [3] formulated a more explicit, temperature rate dependent thermoelasticity, model with two relaxation times.

The dual-phase-lag (DPL) model is proposed by Tzou [4, 5]. The interactions between phonons and electrons on the microscopic level is described as retarding sources causing a delayed response on the macroscopic scale. For macroscopic formulation, it would be convenient to use the DPL mode for investigation of the micro-structural effect on the behavior of heat transfer. The physical meanings and the applicability of the DPL mode have been supported by the experimental results (Tzou [6]).

Many authors have studied the vibration and heat transfer process of beams (Fang et al. [7]). Some of them investigated the thermally-induced displacements and stresses of a rod using the Laplace

*Received by the editors June 10, 2013; Accepted February 2, 2014.
**Corresponding author

transformation technique (Huniti et al. [8]). Others studied the problem of transverse vibrations of a beam induced by a mobile heat source (Kidawa-Kukla [9]). Boley [10], Manolis and Beskos [11], and Rao [12] analyzed the vibrations of a simply supported rectangular beam subjected to a suddenly applied heat or exposed to rapid surface heating or other heat sources. Misra et al. [13] studied the thermoelastic interactions in an elastic half space subjected to a ramp-type heating.

Functionally graded materials (FGMs) are new inhomogeneous materials which have been widely used in many engineering applications such as nuclear reactors and high-speed spacecraft industries [14-19]. The mechanical properties of FGMs vary smoothly and continuously from one surface to the other. Typically these materials are made from a mixture of ceramic and metal or from a combination of different materials. The ceramic constituent of the material provides the high-temperature resistance due to its low thermal conductivity. The ductile metal constituent on the other hand, prevents fracture caused by stresses due to the high temperature gradient in a very short period of time.

The present paper attempts to study the vibration of FG microbeam induced by ramp-type heating in the context of the DPL model. The Laplace transform method is used to determine the lateral vibration, temperature, displacement, stress and its moment, and the strain energy of the microbeam. Numerical results are presented for the FG beam that is subjected to a ramp-type heating and has exponentially varying material properties through the thickness. The effects of the ramping time parameter of thermal vibration and phase lags are studied and represented graphically.

2. BASIC EQUATIONS

The DPL proposed by Tzou [6] is such a modification of the classical thermoelastic model in which the Fourier law is replaced by an approximation to a modified Fourier law with two different time translations: a phase-lag of the heat flux τ_q and a phase-lag of temperature gradient τ_θ. A Taylor series approximation of the modified Fourier law, together with the remaining field equations lead to a complete system of equations describing a dual-phase-lag thermoelastic model. The model transmits thermoelastic disturbance in a wave-like manner if the approximation is linear with respect to τ_q and τ_θ, and $0 \le \tau_\theta < \tau_q$, or quadratic in τ_q and linear in τ_θ, with $\tau_q > 0$ and $\tau_\theta > 0$. This theory is developed in a rational way to produce a fully consistent theory which is able to incorporate thermal pulse transmission in a very logical manner. In equilibrium, the beam is unstrained, unstressed and at temperature T_0 everywhere. If we assume $T(x,z,t)$ to be the transient temperature distribution, the transient temperature change can be defined as $\theta = T - T_0$, assumed to be such that $|\theta / T_0| << 1$.

The DPL model proposed by Tzou [6] is a modification of the classical thermoelastic model in which the Fourier law is replaced by an approximation of the equation:

$$\mathbf{q}(X, t+\tau_q) = -K\nabla\theta(X, t+\tau_\theta) \tag{1}$$

where $\mathbf{q}$ is the heat flux vector, K is thermal conductivity tensor and X is the position vector. The model transmits thermoelastic disturbances in a wave-like manner if Eq. (1) is approximated by

$$\mathbf{q} + \tau_q \frac{\partial \mathbf{q}}{\partial t} + \frac{1}{2}\tau_q^2 \frac{\partial^2 \mathbf{q}}{\partial t^2} = -K\nabla\left(1 + \tau_\theta \frac{\partial}{\partial t}\right)\theta \tag{2}$$

Equation (2) together with the energy balance equation for a rigid heat conductor led to the generalized hyperbolic heat conduction equation. Then, the general heat conduction equation corresponding to the model of thermoelasticity with DPLs takes the form:

$$\left(1+\tau_\theta \frac{\partial}{\partial t}\right)\nabla(K\cdot\nabla\theta)=\left(\delta_1+\delta_2\tau_q\frac{\partial}{\partial t}+\tfrac{1}{2}\delta_3\tau_q^2\frac{\partial^2}{\partial t^2}\right)\left(\rho C^e\frac{\partial\theta}{\partial t}-\rho Q+\gamma T_0\frac{\partial e}{\partial t}\right), \tag{3}$$

where C^e is the specific heat per unit mass at constant strain, ρ is the material density, γ is the stress-temperature modulus, Q is the heat source and $e=\partial u/\partial x+\partial v/\partial y+\partial w/\partial z$ is the volumetric strain. The constitutive equations are given by

$$\sigma_{ij}=2\mu e_{ij}+\lambda e_{kk}\delta_{ij}-\gamma(T-T_0)\delta_{ij}, \tag{4}$$

where σ_{ij} is the stress tensor and δ_{ij} is Kronecker's delta. The strain-displacement relations are given by

$$e_{ij}=\tfrac{1}{2}(u_{i,j}+u_{j,i}). \tag{5}$$

Let us now recall the well-known relations between Lamé's moduli λ, μ and Poisson's ratio ν and Young's modulus E as

$$\lambda=\frac{E\nu}{(1+\nu)(1-2\nu)},\quad \mu=\frac{E}{2(1+\nu)}. \tag{6}$$

Some special cases of thermoelastic theory are given according to the values of all parameters as:

a) Equation of coupled thermoelasticity (CTE) theory

The equations CTE theory are obtained when $\delta_2=\delta_3=\tau_\theta=\tau_q=0$ and $\delta_1=1$.

b) Lord and Shulman's (LS) thermoelasticity theory

For LS theory, $\tau_\theta=0$, $\delta_1=\delta_2=1$, $\delta_3=0$ and $\tau_q=\tau_0>0$ where τ_0 is the first relaxation time.

c) Equations of generalized thermoelasticity with dual phase lag (DPL) theory

The DPL theory is given by setting $\delta_1=\delta_2=1=\delta_3$, $\tau_q>0$ and $\tau_\theta>0$.

3. FORMULATION OF THE PROBLEM

Beams with rectangular cross-sections are mostly employed in MEMS resonators. A micro-resonator can be modeled as an elastic prism beam with either doubly clamped or simply supported ends. Here we consider a thin elastic beam with dimensions of length L $(0\le x\le L)$, width b $(-b/2\le y\le +b/2)$ and thickness h $(-h/2\le z\le +h/2)$. We define the *x*-axis along the axis of the beam and the *y*- and *z*-axes correspond to the width and thickness, respectively. In equilibrium, the beam is unstrained, unstressed and at temperature T_0 everywhere. If we assume $T(x,z,t)$ to be the transient temperature distribution, the transient temperature change can be defined as $\theta=T-T_0$. The formulation of the problem is based on generalized thermoelasticity without energy dissipation.

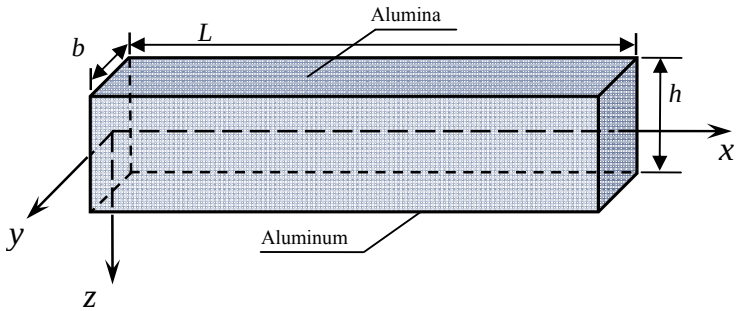

Fig. 1. Schematic diagram for the FG microbeam

A new model of FGMs is presented to treat the governing equations of the thermoelastic microbeam subjected to a ramp-type heating. Based on this model, the effective material property $P(z)$ gradation through the thickness direction is presented by [20, 21]

$$P(z) = P_{\mathrm{m}}\, \mathrm{e}^{n_P(2z-h)/h}, \quad n_P = \ln\sqrt{P_{\mathrm{m}}/P_{\mathrm{c}}}, \tag{7}$$

where P_{m} and P_{c} represent the metal and ceramic properties, respectively. This study assumes that Young's modulus E, material density ρ, thermal conductivity coefficient K and the stress-temperature modulus γ of the FGM change continuously through the thickness direction of the beam according to the gradation relation given in Eq. (7). It is to be noted that the material properties of the considered beam are metal-rich (fully metal) at the lower surface $(z = +h/2)$ and ceramic-rich (fully ceramic) at the upper surface $(z = -h/2)$ of the beam.

The beam undergoes bending vibrations of small amplitude about the *x*-axis such that the deflection is consistent with the linear Euler-Bernoulli theory. That is, any plane cross-section initially perpendicular to axis of beam remains, plane and perpendicular to the neutral surface during bending. Thus the displacements are given by

$$u = -z\frac{\partial w}{\partial x}, \quad v = 0, \quad w(x,y,z,t) = w(x,t), \tag{8}$$

where w is the lateral deflection. Substituting this Euler-Bernoulli assumption into Eq. (8), with the aid of Eq. (7), gives the thermal conduction equation for the beam without the heat source $(Q = 0)$, as

$$K_m\, \mathrm{e}^{n_K(2z-h)/h}\left(1+\tau_\theta\frac{\partial}{\partial t}\right)\left(\frac{\partial^2\theta}{\partial x^2}+\frac{\partial^2\theta}{\partial z^2}+\frac{2n_K}{h}\frac{\partial\theta}{\partial z}\right)=$$

$$=\left(\delta_1+\delta_2\tau_q\frac{\partial}{\partial t}+\frac{1}{2}\delta_3{\tau_q}^2\frac{\partial^2}{\partial t^2}\right)\frac{\partial}{\partial t}\left[\rho_m C_m^e\, \mathrm{e}^{n_{\rho C^e}(2z-h)/h}\,\theta - z\,\mathrm{e}^{n_\gamma(2z-h)/h}\,\gamma_m T_0\frac{\partial^2 w}{\partial x^2}\right], \tag{9}$$

where K_{m}, ρ_{m}, γ_{m} and C_{m}^e are, respectively, the thermal conductivity, the material density, the stress-temperature modulus, and the specific heat per unit mass at constant strain of the metal material. In addition, one gets the relations:

$$\gamma_{\mathrm{m}} = E_{\mathrm{m}}\alpha_{\mathrm{m}}/(1-2\nu_{\mathrm{m}}), \qquad \rho_{\mathrm{m}}C_{\mathrm{m}}^e = K_{\mathrm{m}}/\chi_{\mathrm{m}}, \tag{10}$$

in which E_{m} is Young's modulus, α_{m} is the thermal expansion coefficient, ν_{m} is Poisson's ratio and χ_{m} is the thermal diffusivity, all of the metal material. Note that the parameters n_K, n_γ and $n_{\rho C^e}$ are given in Appendix A.

There is no heat flow across the upper and lower surfaces of the beam (thermally insulated), so that $\partial\theta/\partial z$ should disappear at the upper and lower surfaces of the beam $z = \pm h/2$. For a very thin beam (microbeam), assuming that the temperature increment varies sinusoidally along the thickness direction. That is

$$\theta(x,z,t) = \theta_1(x,t)\sin\left(\tfrac{\pi z}{h}\right). \tag{11}$$

Now, substituting Eq. (11) into Eq. (9) and integrating the resulting equation with respect to z through the beam thickness from $-h/2$ to $h/2$, yields

$$\left(1+\tau_\theta\frac{\partial}{\partial t}\right)\frac{\partial^2\theta_1}{\partial x^2}=\left(\delta_1+\delta_2\tau_q\frac{\partial}{\partial t}+\tfrac{1}{2}\delta_3\tau_q^2\frac{\partial^2}{\partial t^2}\right)\frac{\partial}{\partial t}\left[\overline{\mu}_{\rho C^e}\eta\theta_1-\frac{\overline{\mu}_\gamma T_0 h\gamma_{\mathrm{m}}}{K_{\mathrm{m}}}\frac{\partial^2 w}{\partial x^2}\right], \tag{12}$$

where η, $\overline{\mu}_{\rho C^e}$ and $\overline{\mu}_\gamma$ are given in Appendix A.

The constitutive Eqs. (4) are reduced to the uniaxial tensile stress

$$\sigma_x = -E_{\mathrm{m}}\left(\mathrm{e}^{n_E(2z-h)/h}\, z\frac{\partial^2 w}{\partial x^2} + \alpha_{\mathrm{m}}\, \mathrm{e}^{n_{E\alpha}(2z-h)/h}\, \theta \right), \tag{13}$$

where n_E and $n_{E\alpha}$ are given in Appendix A. The flexure moment of the cross-section is given, with the aid of Eq. (7), by

$$M(x,t) = b\int_{-h/2}^{+h/2} \sigma_x z\,\mathrm{d}\,z = -bh^2 E_{\mathrm{m}}\left(h\mu_E \frac{\partial^2 w}{\partial x^2} + \alpha_{\mathrm{m}}\mu_{E\alpha}\theta_1 \right), \tag{14}$$

where μ_E and $\mu_{E\alpha}$ are given in Appendix A.

The equation of motion for the microbeam is given by

$$\frac{\partial^2 M}{\partial x^2} = \frac{1-\mathrm{e}^{-2n_\rho}}{2n_\rho}\rho_{\mathrm{m}} A\frac{\partial^2 w}{\partial t^2}, \tag{15}$$

where $A = bh$ is the cross-section area. Substituting Eq. (14) into Eq. (15), one can obtain the motion equation as

$$\frac{\partial^4 w}{\partial x^4} + \frac{1-\mathrm{e}^{-2n_\rho}}{2n_\rho \mu_E \varepsilon^2 h^2}\frac{\partial^2 w}{\partial t^2} + \frac{\alpha_m \overline{\mu}_{E\alpha}}{h}\frac{\partial^2 \theta_1}{\partial x^2} = 0, \tag{16}$$

where $\overline{\mu}_{E\alpha} = \mu_{E\alpha}/\mu_E$ and $c = \sqrt{E_{\mathrm{m}}/\rho_{\mathrm{m}}}$.

Now, let us consider the two ends of the microbeam are simply-supported:

$$w(x,t)\big|_{x=0,L} = 0, \qquad \frac{\partial^2 w(x,t)}{\partial x^2}\bigg|_{x=0,L} = 0. \tag{17}$$

Let us also consider the microbeam is loaded thermally by a ramp-type heating incidents into the surface of the microbeam $x = 0$,

$$\theta_1(x,t)\big|_{x=0} = f(t) = \theta_0 \begin{cases} 0 & \text{for} \quad t \le 0, \\ \dfrac{t}{t_0} & \text{for} \quad 0 \le t \le t_0, \\ 1, & \text{for} \quad t > t_0, \end{cases} \tag{18}$$

where t_0 indicates the length of time to rise, the heat is non-negative constant and is called ramp-type parameter and θ_0 is constant, this means that the boundary of the half-space, which is initially at rest and has a fixed temperature T_0, is suddenly raised to a temperature equal to the function $f(t)$ and maintained at this temperature from then on. Considering the aspect of rise of time, various authors investigated many applications in which the ramp-type heating is used [22, 23].

Assuming that the boundary $x = L$ is thermally insulated, there is no variation of the temperature on it. This means that the following relation will be satisfied

$$\frac{\partial \theta_1}{\partial x} = 0 \quad \text{on} \quad x = L. \tag{19}$$

The governing equations can be put in the dimensionless forms using the following parameters:

$$(x', L', u', w', z', h') = \eta\varepsilon(x, L, u, w, z, h), \quad (t', t_0') = \eta\varepsilon^2(t, t_0),$$
$$\theta_1' = \frac{\theta_1}{T_0}, \quad \sigma_x' = \frac{\sigma_x}{E_m}, \quad M' = -\frac{M}{bh^3 E_m \mu_E \eta\varepsilon}. \tag{20}$$

So, the governing equations and the bending and stress are simplified as (dropping the primes for convenience)

$$\frac{\partial^4 w}{\partial x^4} + A_1 \frac{\partial^2 w}{\partial t^2} + A_2 \frac{\partial^2 \theta_1}{\partial x^2} = 0,$$
$$\left(1 + \tau_\theta \frac{\partial}{\partial t}\right)\frac{\partial^2 \theta_1}{\partial x^2} = \left(\delta_1 + \delta_2 \tau_q \frac{\partial}{\partial t} + \tfrac{1}{2}\delta_3 \tau_q^2 \frac{\partial^2}{\partial t^2}\right)\frac{\partial}{\partial t}\left[A_3 \theta_1 - A_4 \frac{\partial^2 w}{\partial x^2}\right], \tag{21}$$

$$M = \frac{\partial^2 w}{\partial x^2} + A_2 \theta_1, \tag{22}$$

$$\sigma_x = \mathrm{e}^{n_E(2z-h)/h} \frac{\partial u}{\partial x} - A_5\, \mathrm{e}^{n_{E\alpha}(2z-h)/h} \sin\left(\frac{\pi z}{h}\right)\theta_1, \tag{23}$$

where

$$A_1 = \frac{1 - \mathrm{e}^{-2n_\rho}}{2n_\rho \mu_E h^2}, \; A_2 = \frac{\alpha_{\mathrm{m}} \overline{\mu}_{E\alpha} T_0}{h}, \; A_3 = \overline{\mu}_{\rho C^e}, \; A_4 = \frac{\overline{\mu}_\gamma h \gamma_{\mathrm{m}}}{\eta K_{\mathrm{m}}}, \; A_5 = \alpha_{\mathrm{m}} T_0. \tag{24}$$

If the thermoelastic coupling effect is disregarded $(A_4 = 0)$, the governing equations consisting of the non-Fourier thermal conduction equation and the motion equation of the beam can be expressed as

$$\frac{\partial^4 w}{\partial x^4} + A_1 \frac{\partial^2 w}{\partial t^2} + A_2 \frac{\partial^2 \theta_1}{\partial x^2} = 0,$$
$$\left(1 + \tau_\theta \frac{\partial}{\partial t}\right)\frac{\partial^2 \theta_1}{\partial x^2} = A_3\left(\delta_1 + \delta_2 \tau_q \frac{\partial}{\partial t} + \tfrac{1}{2}\delta_3 \tau_q^2 \frac{\partial^2}{\partial t^2}\right)\frac{\partial \theta_1}{\partial t}. \tag{25}$$

Comparing Eq. (21) with Eq. (25) shows that it is much more difficult to solve the governing equation of the CTE case than to solve that of the uncoupled case.

4. SOLUTION IN THE LAPLACE TRANSFORM DOMAIN

In order to solve the problem, both the initial and boundary conditions should be considered. The initial conditions of the problem are taken as

$$w(x,t)\big|_{t=0} = \left.\frac{\partial w(x,t)}{\partial t}\right|_{t=0} = 0, \quad \theta_1(x,t)\big|_{t=0} = \left.\frac{\partial \theta_1(x,t)}{\partial t}\right|_{t=0} = 0. \tag{26}$$

The closed form solution of the governing and constitutive equations may be possible by adapting the Laplace transformation method. Applying the Laplace transform to Eqs. (21), one gets the field equations in the Laplace transform space as

$$\frac{\mathrm{d}^4 \overline{w}}{\mathrm{d}x^4} + A_1 s^2 \overline{w} + A_2 \frac{\mathrm{d}^2 \overline{\theta}_1}{\mathrm{d}x^2} = 0,$$
$$\left(1 + \tau_\theta s\right)\frac{\mathrm{d}^2 \overline{\theta}_1}{\mathrm{d}x^2} = s\left(\delta_1 + \delta_2 \tau_q s + \tfrac{1}{2}\delta_3 \tau_q^2 s^2\right)\left(A_3 \overline{\theta}_1 - A_4 \frac{\mathrm{d}^2 \overline{w}}{\mathrm{d}x^2}\right), \tag{27}$$

where an over bar symbol denotes its Laplace transform, s denotes the Laplace transform parameter. Eliminating $\overline{\theta}_1$ or $\overline{w}$ from Eqs. (27) gives the following differential equation for $\overline{w}$ or $\overline{\theta}_1$:

$$\left[\frac{\mathrm{d}^6}{\mathrm{d}x^6} - A\frac{\mathrm{d}^4}{\mathrm{d}x^4} + B\frac{\mathrm{d}^2}{\mathrm{d}x^2} - C\right]\{\overline{w}, \overline{\theta}_1\} = 0, \tag{28}$$

where the coefficients A, B and C are given by

$$A = \frac{s\left(\delta_1 + \delta_2\tau_q s + \frac{1}{2}\delta_3\tau_q^2 s^2\right)(A_3 + A_2A_4)}{1+\tau_\theta s},\ B = A_1 s^2,\ \ C = \frac{\left(\delta_1 + \delta_2\tau_q s + \frac{1}{2}\delta_3\tau_q^2 s^2\right)A_1A_3 s^3}{1+\tau_\theta s}. \tag{29}$$

Eq. (28) can be factorized into the following equation

$$(D^2 - m_1^2)(D^2 - m_2^2)(D^2 - m_3^2)\{\overline{w}, \overline{\theta}_1\} = 0, \tag{30}$$

where $D = \mathrm{d}/\mathrm{d}x$ and m_1^2, m_2^2 and m_3^2 are the roots of the characteristic equation

$$m^6 - Am^4 + Bm^2 - C = 0. \tag{31}$$

These roots are given by

$$\begin{gathered} m_1^2 = \tfrac{1}{3}[2p_0\sin(q_0) + A],\quad m_2^2 = -\tfrac{1}{3}p_0[\sqrt{3}\cos(q_0) + \sin(q_0)] + \tfrac{1}{3}A, \\ m_3^2 = \tfrac{1}{3}p_0[\sqrt{3}\cos(q_0) - \sin(q_0)] + \tfrac{1}{3}A, \end{gathered} \tag{32}$$

where

$$p_0 = \sqrt{A^2 - 3B},\quad q_0 = \tfrac{1}{3}\sin^{-1}\left(-\frac{2A^3 - 9AB + 27C}{2p_0^3}\right). \tag{33}$$

The solution of the governing equations, Eqs. (28) in the Laplace transformation domain can be represented as

$$\{\overline{w}, \overline{\theta}_1\} = \sum_{i=1}^{3}\left(\{C_i, F_i\}\mathrm{e}^{-m_i x} + \{C_{i+3}, F_{i+3}\}\mathrm{e}^{m_i x}\right), \tag{34}$$

where C_i and F_i are parameters depending on s. The compatibility between these two equations and Eqs. (28), gives

$$F_i = \beta_i C_i,\quad F_{i+3} = \beta_i C_{i+3},\quad \beta_i = -\frac{m_i^4 + A_1 s^2}{A_2 m_i^2}. \tag{35}$$

So,

$$\overline{\theta}_1 = \beta_i\overline{w} = \sum_{i=1}^{3}\beta_i\left(C_i\,\mathrm{e}^{-m_i x} + C_{i+3}\,\mathrm{e}^{m_i x}\right) \tag{36}$$

Then, the bending moment M and stress σ_x given in Eqs. (20) and (21) in the Laplace domain with the aid of the above equation, become

$$\overline{M} = \sum_{i=1}^{3}\left(m_i^2 + A_2\beta_i\right)\left(C_i\,\mathrm{e}^{-m_i x} + C_{i+3}\,\mathrm{e}^{m_i x}\right), \tag{37}$$

$$\overline{\sigma}_x = -\sum_{i=1}^{3}[zm_i^2 + A_5\beta_i\sin(\pi z/h)]\left(C_i\,\mathrm{e}^{-m_i x} + C_{i+3}\,\mathrm{e}^{m_i x}\right) \tag{38}$$

Also, the axial displacement after using Eq. (32) takes the form

$$\overline{u} = -z\frac{\mathrm{d}\overline{w}}{\mathrm{d}x} = z\sum_{i=1}^{3} m_i\left(C_i\,\mathrm{e}^{-m_i x} - C_{i+3}\,\mathrm{e}^{m_i x}\right) \tag{39}$$

In addition, the strain will be

$$\overline{e} = \frac{\mathrm{d}\overline{u}}{\mathrm{d}x} = -z\sum_{i=1}^{3} m_i^2\left(C_i\,\mathrm{e}^{-m_i x} + C_{i+3}\,\mathrm{e}^{m_i x}\right) \tag{40}$$

Note that, the strain energy which is generated on the beam is given, after using Laplace transform, by

$$\overline{W} = \tfrac{1}{2}\sum_{i,j=1}^{3} \overline{\sigma}_{ij}\overline{e}_{ij} = \tfrac{1}{2}\overline{\sigma}_x\overline{e}. \tag{41}$$

Note that, after using Laplace transform, the boundary conditions take the forms

$$\begin{aligned} &\overline{w}(x,s)\big|_{x=0,L} = 0, \quad \left.\frac{\mathrm{d}^2\,\overline{w}(x,s)}{\mathrm{d}\,x^2}\right|_{x=0,L} = 0, \\ &\overline{\theta}_1(x,s)\big|_{x=0} = \frac{\theta_0}{t_0}\left(\frac{1-e^{-st_0}}{s^2}\right) = \overline{G}(s), \quad \left.\frac{\mathrm{d}\,\overline{\theta}_1(x,s)}{\mathrm{d}\,x}\right|_{x=L} = 0. \end{aligned} \tag{42}$$

Substituting Eqs. (36) into the above boundary conditions gives

$$[F][C] = [D], \tag{43}$$

where

$$[F] = \begin{bmatrix} 1 & 1 & 1 & 1 & 1 & 1 \\ \mathrm{e}^{-m_1 L} & \mathrm{e}^{-m_2 L} & \mathrm{e}^{-m_3 L} & \mathrm{e}^{m_1 L} & \mathrm{e}^{m_2 L} & \mathrm{e}^{m_3 L} \\ \beta_1 m_1^2 & \beta_2 m_2^2 & \beta_3 m_3^2 & \beta_1 m_1^2 & \beta_2 m_2^2 & \beta_3 m_3^2 \\ \beta_1 m_1^2\,\mathrm{e}^{-m_1 L} & \beta_2 m_2^2\,\mathrm{e}^{-m_2 L} & \beta_3 m_3^2\,\mathrm{e}^{-m_3 L} & \beta_1 m_1^2 e^{m_1 L} & \beta_2 m_2^2\,\mathrm{e}^{m_2 L} & \beta_3 m_3^2\,\mathrm{e}^{m_3 L} \\ \beta_1 & \beta_2 & \beta_3 & \beta_1 & \beta_2 & \beta_3 \\ -m_1\beta_1\,\mathrm{e}^{-m_1 L} & -m_2\beta_2\,\mathrm{e}^{-m_2 L} & -m_3\beta_3\,\mathrm{e}^{-m_3 L} & m_1\beta_1\,\mathrm{e}^{m_1 L} & m_2\beta_2\,\mathrm{e}^{m_2 L} & m_3\beta_3\,\mathrm{e}^{m_3 L} \end{bmatrix},$$

$$[C] = \left[C_1, C_2, C_3, C_4, C_5, C_6\right]^T \text{ and } [D] = \left[0,0,0,0,\overline{G}(s),0\right]^T.$$

The unknown parameters C_i and C_{i+3}, $i = 1,2,3$ can be obtained by solving Eq. (43). This completes the solution of the problem in the Laplace transform domain.

5. NUMERICAL INVERSION OF THE LAPLACE-TRANSFORMED EQUATIONS

To obtain a solution of the problem in the physical domain, the transforms in Eqs. (36)-(41) are inverted. In order to invert the Laplace transform in the above equations, we adopt a numerical inversion method based on a Fourier series expansion [24]. In this method, any function in Laplace domain can be inverted to the time domain as

$$\psi(t) = \frac{e^{ct}}{t}\left(\frac{\overline{\psi}(c)}{2} + \mathrm{Re}\sum_{n=1}^{N}\overline{\psi}(c + in\pi/t)(-1)^n\right),$$

where Re is the real part and i is imaginary number unit. For faster convergence, numerous numerical experiments have shown that the value of c satisfies the relation $ct \approx 4.7$ [25].

6. NUMERICAL RESULTS AND DISCUSSION

With a view to illustrating the analytical procedure presented earlier, we now consider a numerical example for which computational results are given. The results depict the variations of the non-dimensional lateral vibration, temperature, displacement, stress, moment and strain energy distribution in the context of DPL theory. The aluminum as lower metal surface and alumina as upper ceramic surface are used for the present microbeam. The material properties are assumed to be as:

Metal (aluminum):

$$\begin{aligned} &E_{\mathrm{m}} = 70\ \mathrm{GPa}, \quad \nu_{\mathrm{m}} = 0.35, \quad \rho_{\mathrm{m}} = 2700\ \mathrm{Kg/m^3}, \\ &\alpha_{\mathrm{m}} = 23.1\times10^{-6}\ /\mathrm{K}, \quad K_{\mathrm{m}} = 237\ \mathrm{W/(m\,K)}. \end{aligned}$$

Ceramic (alumina):

$$E_c = 116 \text{ GPa}, \quad \nu_c = 0.33, \quad \rho_c = 3000 \text{ Kg/m}^3,$$
$$\alpha_c = 8.7\times10^{-6} \text{/K}, \quad K_c = 1.78 \text{ W/(m K)}.$$

The reference temperature of the microbeam is $T_0 = 293$ K. The aspect ratios of the beam are fixed as $L/h = 10$. The figures were prepared by using the dimensionless variables which are defined in Eq. (20) for a wide range of beam length when $L = 1$. The computations were carried out for $t = 0.12$ sec and $\theta_0 = 1$. Numerical analysis has been carried out by taking range x from 0.0 to 1.0. The results are depicted in different figures in order to show the variation of different fields with respect to the x coordinate. The numerical results are obtained and presented graphically in Figs. 2-4.

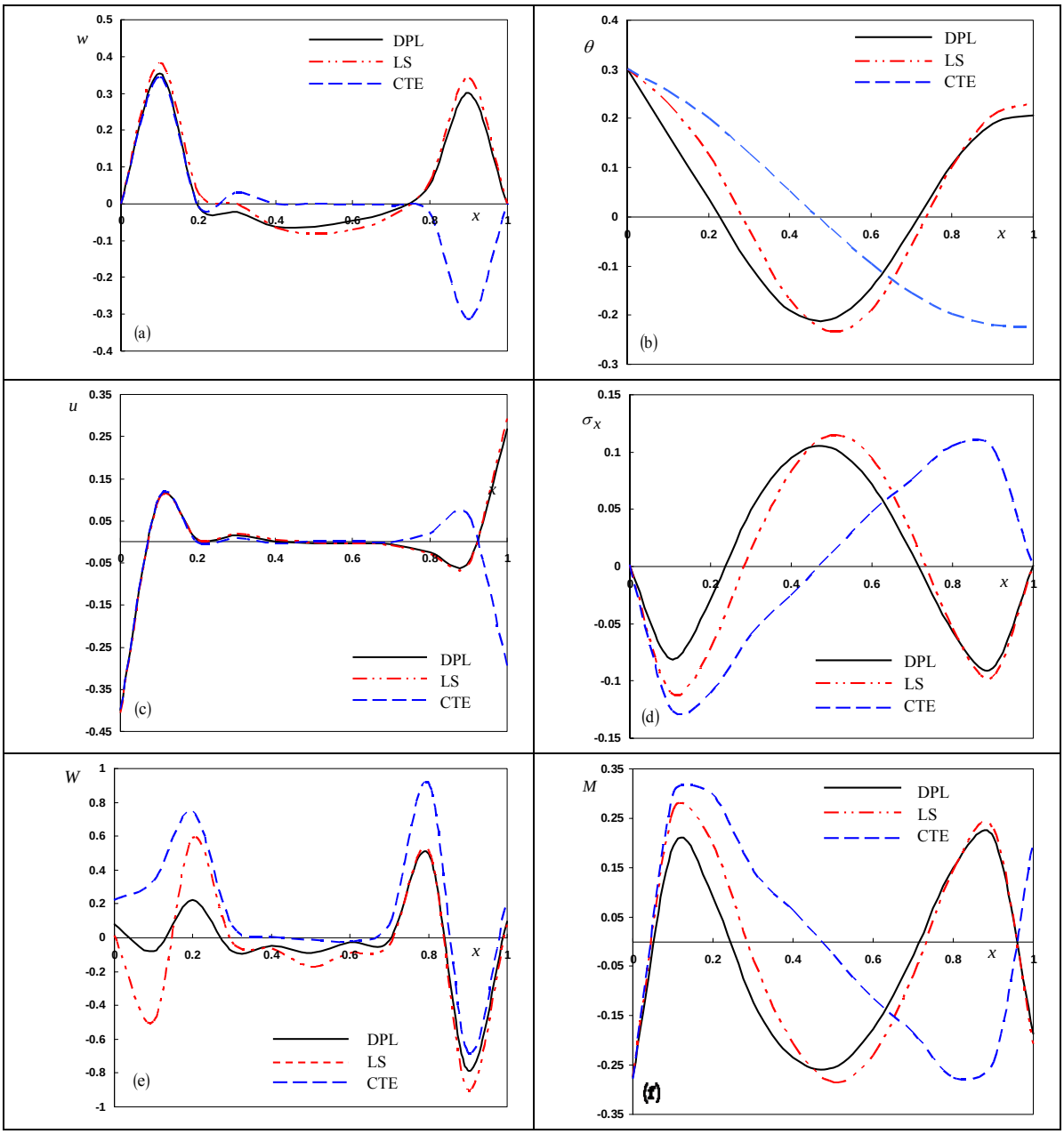

Fig. 2. (a) The transverse deflection, (b) the temperature, (c) the displacement, (d) the thermal stress, (e) the strain energy and (f) the bending moment, distributions of the FG microbeam for different values of DPLs $(z = h/6,\ t = 0.12,\ t_0 = 0.2)$.

Figures 2a to 2f are drawn to give comparison of the results obtained for the non-dimensional lateral vibration, temperature, displacement, stress, moment and strain energy at $t_0 = 0.2$. The graphs in Figs. 2a to 2f represent six curves predicted by three different theories of thermoelasticity obtained as a special case of the DPL model. The computations were performed for one value of time, namely for $t = 0.12$ and various values of the parameters τ_q and τ_θ. The values of τ_q and τ_θ can judge whether the wavelike behavior in the DPL heat conduction is dominant or not. However, it can be found from the numerical results that the shift times τ_q and τ_θ may play a more important role in this task.

Figure 2a depicts the distribution of the lateral vibration w through the length of the beam when the ramping time parameter t_0 remains constant. It always begins at the zero value and non-uniformly vibrates through the beam length to vanish once again at the end of the beam. This satisfies the boundary condition at beam boundaries. The behavior of CTE model may be different from those of LS and DPL models. The peak values of non-dimensional lateral vibration occurs near the ends of the microbeam at $x = 0.1$ and $x = 0.9$, respectively.

Figure 2b shows that the temperature θ decreases as the axial distance x increases to move in the direction of wave propagation in the range $0 \le x \le 0.45$ and then it increases. This disturbance may be due to the thermally loaded (ramp-type heating) incidents into the surface of the microbeam. The temperature of CTE model may differ from those of the other theories.

Figure 2c suggests that the axial displacement u moves directly in the direction of wave propagation. Once again, the behavior of CTE model may be different from those of LS and DPL models near the beam end only $(x = L)$. The axial displacement attains a stationary maximum value at $x \cong 0.2$.

Figure 2d plots the axial stress σ_x of the FG microbeam when the ramping time parameter t_0 remains constant. In fact, the given stress σ_x is changed to positive first and achieves its maximum at $x = 0.45$ in the cases of LS and DPL models. In the case of CTE model, the stress sσ_x reaches its maximum at $x = 0.9$.

Figure 2e shows that the strain energy W of the microbeam obtains different behaviors according to the models used. The values in classical theory of thermoelasticity (CTE model) are quite similar compared to those of other theories. The strain energy W may be moved in the direction of wave propagation through the beam length.

Figure 2f investigates the non-dimensional bending moment M predicted by the three different theories of thermoelasticity. The behavior of LS model is completely different from that of CTE model.

In Figs. 3a to 3f, the DPL model is used to investigate the non-dimensional lateral vibration, temperature, displacement, stress, moment and strain energy for different values of the ramping time parameter t_0. In order to observe the effect of the parameter t_0 on the values of different field variables we carry out our computation for three different non zero values of the parameter t_0 (0.2, 0.4, 0.6). Some values for the field quantities are computed for $z = h/6$ with different values of x. The field quantities such as temperature, stress and displacement depend not only on the state and space variables t and x, but also on rise-time parameter t_0. It has been observed in Figs. 3a to 3f that, the finite rise-time parameter plays a vital role on the development of all the studied fields. The increase in the value of the ramping time parameter causes decreasing in the values of all the fields, which is very obvious in the peak points of the curves. Also, the damping of the strain energy is increased when the ramping time parameter increases. In most of the earlier studies, mechanical or thermal loading on the bounding surface is considered to be in the form of a shock. However, the sudden jump of the load is merely an idealized situation because it is impossible to realize a pulse described mathematically by a step function; even very rapid rise-time (of the order of 10^{-9} s) may be slow in terms of the continuum.

Figures 4a to 4f present, in three dimensions, the temperature, displacement, stress, strain, and the strain energy of the beam at constant value of the ramping time parameter $t_0 = 0.4$ and wide range of

thickness $-1/2 \le z/h \le 1/2$. In those figures, the effects of the changing of the thickness on all the studied fields are pronounced. When the thickness increases the values of all the studied fields increase and it is very obvious at the peak points of the curves. It is concluded that different gradient parameters produce different distributions of the thermal stresses.

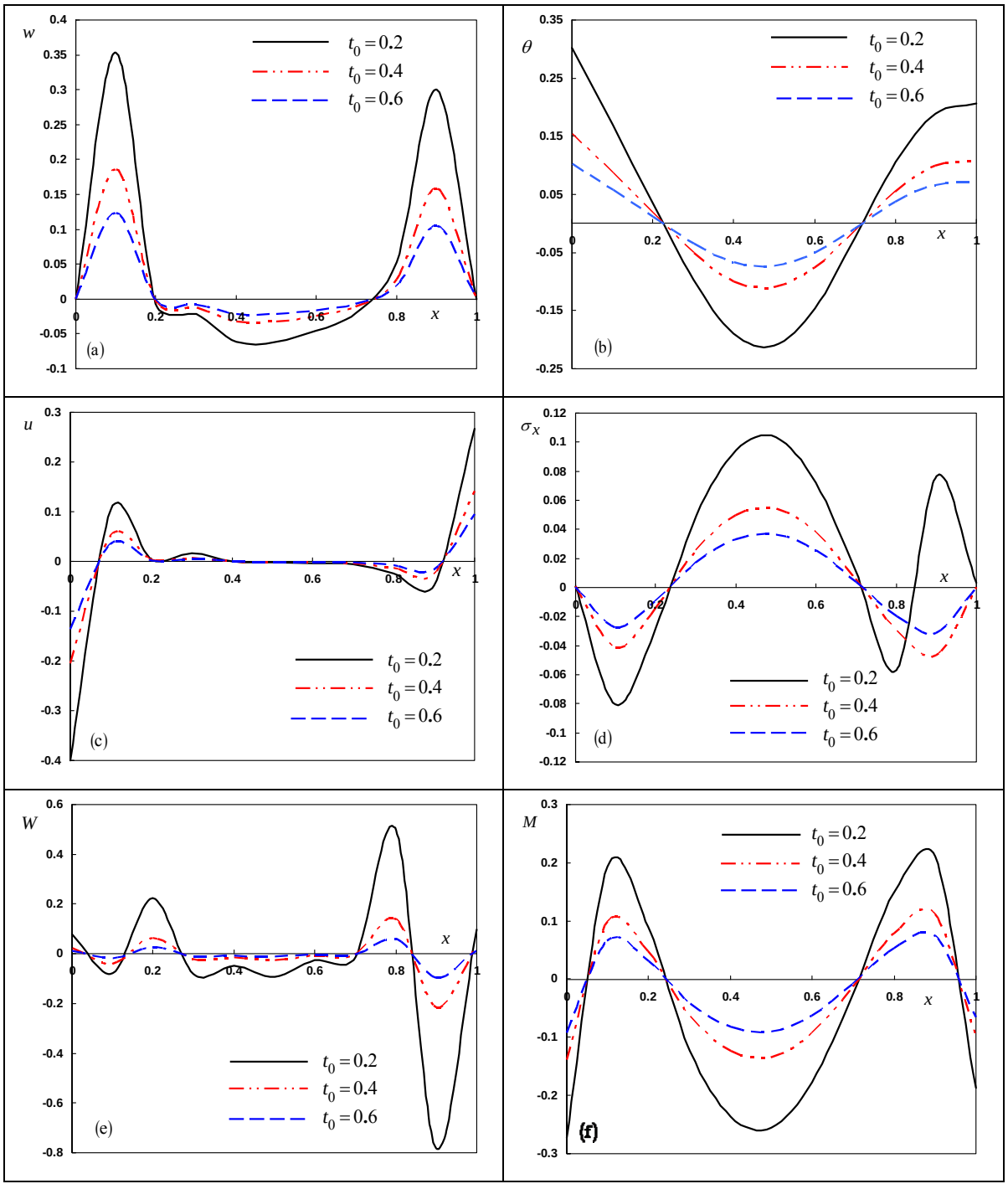

Fig. 3. The effect of the ramping time parameter on (a) the transverse deflection, (b) the temperature, (c) the displacement, (d) the thermal stress, (e) the strain energy and (f) the bending moment, distributions of the FG microbeam $(z = h/6,\ t = 0.12,\ a = 0.01)$.

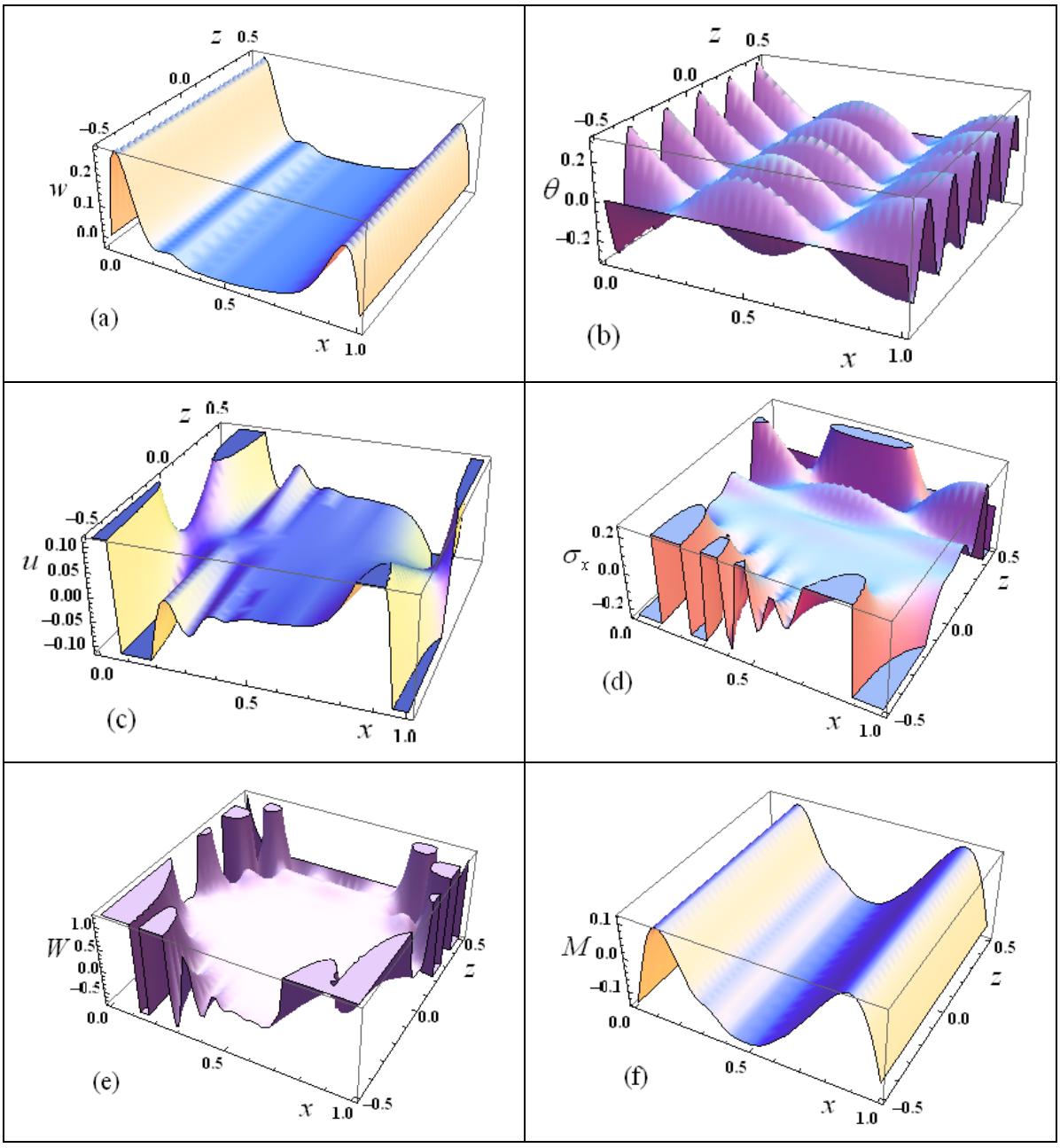

Fig. 4. (a) The transverse deflection, (b) the temperature, (c) the displacement, (d) the thermal stress, (e) the strain energy and (f) the bending moment versus the axial and thickness directions $(t = 0.12,\ t_0 = 0.2)$

7. CONCLUSION

In this work, the influence of the non-Fourier effect on heat transfer and the thermoelastic wave is studied. When very fast phenomena and small structure dimensions are involved, the classical law of Fourier becomes inaccurate. A more sophisticated model is then needed to describe the thermal conduction mechanisms in a physically acceptable way. Modern technology has enabled the fabrication of materials and devices with characteristic dimensions of a few micrometers. Examples are super lattices, micro-wires, and quantum dots. At these length scales, the familiar continuum Fourier law for heat conduction is

expected to fail due to both classical and quantum size effects [26]. A model of generalized thermoelasticity with DPLs for an elastic FG microbeam is constructed.

The Laplace transform technique is used to obtain the general solution for any set of boundary conditions. The exact solution of the generalized thermoelasticity theory governing equations for a coupled and nonlinear/linear exists only for very special and simple initial and boundary problem. In view of calculating general problems, a numerical solution technique is to be used. For this reason the Laplace transform technique is chosen.

The general solutions are applied to a specific problem of an Euler–Bernoulli microbeam induced by a ramp-type heating. The inverse Laplace transforms are computed numerically, and the comparisons are shown in figures to estimate the effects of the thickness and the ramping time parameter on all the studied fields. A comparison is made with the results predicted by the three theories.

The following conclusions can be obtained based on the above analysis:

- The ramping time parameter has a significant effect on the field quantities.
- The PLs have a great effect on the distribution of field.
- Our results indicate that the thermal stresses can be relaxed for some specified gradients. In engineering application, this feature permits one to choose appropriate gradients to make the FG beams safe in structural integrity when subjected to high-temperature change of the inner or outer environment.
- The method used in the present article is applicable to a wide range of problems in thermodynamics and thermoelasticity.
- Results obtained in this paper may be considered as more general in the sense that they include the combined effect of graded and an ramping time heating.
- Physical applications are found in the mechanical engineering, geophysical, and industrial sectors.
- The theories of coupled thermoelasticity (CTE) and generalized thermoelasticity with one relaxation time (LS) can be extracted as special cases.
- There are significant differences for field quantities under the three theories due to essential differences between the CTE theory CTE, the LS theory and DPL theory.
- The distribution in LS theory is near to that in DPL theory, whereas the distributions in the CTE theory are different from that in DPL theory. This is in agreement with [27] in which the DPL model is an extension of the LS model.

REFERENCES

1. Biot, M. A. (1956). Thermoelasticity and irreversible thermodynamics. *J. Appl. Phys.*, Vol. 27, pp. 240–253.
2. Lord, H. & Shulman, Y. (1967). A generalized dynamical theory of thermoelasticity. *J. Mech. Phys. Solid,* Vol. 15, pp. 299–309.
3. Green, A. E. & Lindsay, K. A. (1972). Thermoelasticity. *J. Elast.*, Vol. 2, pp. 1–7.
4. Tzou, D. Y. (1995). A unified approach for heat conduction from macro-to micro-scales. *J. Heat Transfer*, Vol. 117, pp. 8–16.
5. Tzou, D. Y. (1996). *Macro-to-microscale heat transfer: the lagging behavior*. Washington, DC, Taylor & Francis.
6. Tzou, D. Y. (1995). Experimental support for the Lagging behavior in heat propagation. *J. Thermophys Heat Trans*, Vol. 9, pp. 686–693.
7. Fang, D. N., Sun, Y. X. & Soh, A. K. (2006). Analysis of frequency spectrum of laser-induced vibration of microbeam resonators. *Chinese Phys. Letter*, Vol. 23, pp. 1554–1557.

8. Al-Huniti, N. S., Al-Nimr, M. A. & Naij, M. (2001). Dynamic response of a rod due to a moving heat source under the hyperbolic heat conduction model. *J. Sound Vib*., Vol. 242, pp. 629–640.
9. Kidawa-Kukla, J. (2003). Application of the green functions to the problem of the thermally induced vibration of a beam. *J. Sound Vib*., Vol. 262, pp. 865–876.
10. Boley, B. A. (1972). Approximate analyses of thermally induced vibrations of beams and plates. *J, Appl. Mech*., Vol. 39, pp. 212–216.
11. Manolis, G. D. & Beskos, D. E. (1980). Thermally induced vibrations of beam structures. *Comput. Meth. Appl. Mech. Eng*., Vol. 21, pp. 337–355.
12. Rao, J. S. (1992). *Advanced theory of vibration: (Nonlinear vibration and one dimensional structures)*. Wiley, New York.
13. Misra, J. C., Chattopadhyay, N. C. & Samanta, S. C. (1996). Study of the thermoelastic interactions in an elastic half space subjected to a ramp-type heating—a state-space approach. *Int. J. Eng. Sci*., Vol. 34, No. 5, pp. 579–596.
14. Yamanouchi, M., Koizumi, M. & Shiota, I. (1990). *Proc. First Int. Symp. Functionally Gradient Materials*, Sendai, Japan.
15. Erdogan, F. (1995). Fracture mechanics of functionally graded materials. *Compos. Eng*., Vol. 5, No. 7, pp. 753–770.
16. Aboudi, J., Pindera, M. J. & Arnold, S. M. (1995). Thermo-inelastic response of functionally graded composites. *Int. J. Solids Struct*., Vol. 32, pp. 1675–1710.
17. Wetherhold, R. C. & Wang, S. S. (1996). The use of functionally graded materials to eliminate or control thermal deformation. *Compos. Sci. Tech.*, Vol. 56, pp. 1099–1104.
18. Lee, W. Y., Stinton, D. P., Berndt, C. C., Erdogan, F., Lee, Y. D. & Mutasim, Z. (1996). Concept of functionally graded materials for advanced thermal barrier coating applications. *J. Am. Ceram. Soc*., Vol. 79, No. 12, pp. 3003–3012.
19. Suresh, S. & Mortensen, A. (1998). *Fundamentals of functionally graded materials*. Inst Mater Commun Ltd, London.
20. Zenkour, A. M. (2007). Elastic deformation of the rotating functionally graded annular disk with rigid casing. *J. Mater. Sci.*, Vol. 42, No. 23, pp. 9717–9724.
21. Zenkour, A. M. (2009). Stress distribution in rotating composite structures of functionally graded solid disks. *J. Mater. Processing Tech.*, Vol. 209, No. 7, pp. 3511–3517.
22. Misra, J. C., Samanta, S. C. & Chakrabarti, A. K. (1991). Magnetothermoelastic interaction in an aeolotropic solid cylinder subjected to a ramp-type heating. *Int. J. Eng. Sci*., Vol. 29, pp. 1065–1075.
23. Abouelregal, A. E. (2011). Fractional order generalized thermo-piezoelectric semi-infinite medium with temperature-dependent properties subjected to a ramp-type heating, *J. Thermal Stresses*, Vol. 34, No. 11, pp. 1139–1155.
24. Hanig, G. & Hirdes, U. (1984). A method for the numerical inversion of Laplace transform. *J. Comp. Appl. Math.*, Vol. 10, pp. 113–132.
25. Tzou, D. (1996). *Macro-to-micro heat transfer*. Taylor & Francis, Washington, D. C.
26. Rao, J. S. (1992). *Advanced theory of vibration (Nonlinear vibration and one dimensional structures)*. Wiley, New York, Chichester, Brisbane, Toronto, Singapore.
27. Hetnarski, R. B. & Ignaczak, J.(1999). Generalized thermoelasticity. *J. Thermal Stresses*, Vol. 22, pp. 451–476.

APPENDIX A

The parameters n_K, n_γ and $n_{\rho C^e}$ appearing in Eq. (9) are given according to Eq. (1) as

$$n_K = \ln\sqrt{K_{\mathrm{m}}/K_{\mathrm{c}}}, \quad n_\gamma = \ln\sqrt{\gamma_{\mathrm{m}}/\gamma_{\mathrm{c}}}, \quad n_{\rho C^e} = \ln\sqrt{\rho_{\mathrm{m}} C^e_{\mathrm{m}}/\rho_{\mathrm{c}} C^e_{\mathrm{c}}},$$

where K_{c}, ρ_{c}, γ_{c} and C_{c}^{e} are, respectively, the thermal conductivity, the material density, the stress-temperature modulus, and the specific heat per unit mass at constant strain, of the ceramic material.
Equation (12) gives $\eta = \rho_{\mathrm{m}} C_{\mathrm{m}}^{e} / K_{\mathrm{m}}$, $\overline{\mu}_{\rho C^e} = \mu_{\rho C^e} / \mu_K$ and $\overline{\mu}_{\gamma} = \mu_{\gamma} / \mu_K$, where

$$\mu_K = \frac{2n_K(1+\mathrm{e}^{-2n_K})}{\pi^2 + 4n_K^2},\ \mu_{\rho C^e} = \frac{2n_{\rho C^e}(1+\mathrm{e}^{-2n_{\rho C^e}})}{\pi^2 + 4n_{\rho C^e}^2},\ \mu_{\gamma} = \frac{n_{\gamma}(1+\mathrm{e}^{-2n_{\gamma}}) - 1 + \mathrm{e}^{-2n_{\gamma}}}{4n_{\gamma}^2}.$$

The parameters n_E and $n_{E\alpha}$ appearing in Eq. (13) are given by

$$n_E = \ln\sqrt{E_{\mathrm{m}} / E_{\mathrm{c}}},\quad n_{E\alpha} = \ln\sqrt{E_{\mathrm{m}}\alpha_{\mathrm{m}} / E_{\mathrm{c}}\alpha_{\mathrm{c}}},$$

in which α_{c} and E_{c} are the thermal expansion coefficient and Young's modulus of the ceramic material, respectively.

The coefficicents μ_E and $\mu_{E\alpha}$ appearing in Eq. (14) are given by

$$\mu_E = \frac{(n_E^2 + 2)(1-\mathrm{e}^{-2n_E}) - 2n_E(1+\mathrm{e}^{-2n_E})}{8n_E^3},$$

$$\mu_{E\alpha} = \frac{n_{E\alpha}(4n_{E\alpha}^2 + \pi^2)(1-\mathrm{e}^{-2n_{E\alpha}}) + (\pi^2 - 4n_{E\alpha}^2)(1+\mathrm{e}^{-2n_{E\alpha}})}{(\pi^2 + 4n_{E\alpha}^2)^2}.$$